

## A Thresholding Approach for Segmenting Deteriorated SEM Images in an Automated X-ray Mask Visual Inspection System

Minoru Ito  
Dept. of Electronic Engineering  
Kogakuin University

1-24-2, Nishi-Shinjuku, Shinjuku-ku, Tokyo, 163-91 Japan

### ABSTRACT

The most troublesome problem in automated X-ray mask inspection is how to exactly determine the threshold level for extracting the pattern portions of each scanning electron microscopic (SEM) image. An exact determination is difficult because the histogram shows, in most cases, a complicated multi-modal pattern and the true threshold level often varies too much with each successive image to be deduced from threshold values determined for the preceding image. This paper presents a novel thresholding approach for segmenting SEM images of X-ray masks. In this approach, the shape of the histogram of each image is iteratively analyzed until a reliable threshold value satisfying all criteria for determining thresholds is obtained. This new approach is used in an automated inspection system. When the input image resolution is set to  $0.05 \mu\text{m}/\text{pixel}$ , experiments confirm  $0.1 \mu\text{m}$  defects are unfaillingly detected.

### 1 INTRODUCTION

Automated X-ray mask inspection is indispensable for certifying the quality of X-ray masks used in the production of LSIs with sub-quarter micron patterns on the order of  $0.2 \mu\text{m}$  wide, which will be used for next-generation memories of more than 256 Mbit [1]. The mask used in the SOR (Synchrotron Orbital Radiation) lithography is a silicon nitride thin film a few microns in thickness that is transparent for SOR [2]. The fine patterns on the mask are made of a heavy metal such as tantalum, which prevents SOR from passing through the mask [3]. The minimum size of patterns drawn on the X-ray mask is  $0.2 \mu\text{m}$ . This is much smaller than the patterns on the conventional optical mask, or reticule, used in optical lithography. The optical microscopes used in conventional inspection are not suitable for X-ray mask inspection any longer because their resolution is limited to  $0.4 \mu\text{m}$  at best [4].

The most practical way to inspect X-ray masks is by SEM (Scanning Electron Microscope) because of its high resolution. However, in SEM images, there is a large non-uniformity of output-signal levels due to non-uniform electron charge-up on the mask and the output-signal levels on pattern edges is very high due to the edge effect [5]. The most difficult problem in X-ray mask inspection is how to exactly determine the threshold level for extracting the pattern por-

tions of such a deteriorated SEM images. An exact determination is difficult because the histogram shows, in most cases, a complicated multi-modal pattern and the true threshold level, due to dominant nonuniformity of electron charge-up on the mask, often varies too much with each successive image to be deduced from threshold values determined for the preceding image. This difficulty has so far prevented us from developing an automated X-ray mask inspection system where mask patterns are compared with their corresponding design data.

This paper presents a novel thresholding approach for segmenting SEM images of X-ray masks. The shape of the histogram of each image is iteratively analyzed until a reliable threshold value satisfying all criteria for determining thresholds is obtained. Experiments confirm fine defects as small as  $0.05 \mu\text{m}$  on X-ray mask patterns can be unfaillingly detected on the basis of chip-to-CAD comparison where input SEM images are compared with their corresponding design data.

### 2 OVERVIEW OF INSPECTION SYSTEM

The system hardware configuration is shown in Fig. 1. A SEM with a spatial resolution higher than 20 nm is used to generate analog image signals of a mask pattern. The image resolution in the inspection mode is usually 25 or 50 nm/pixel. The AD processor (ADP) does low-level image processing such as the correction of image magnification and rotation relative to the corresponding design data. The defect detection processor (UIP) detects significant mask defects in the images sent from the ADP. Its main jobs

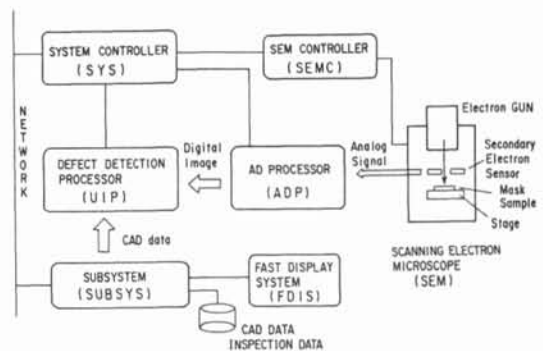


Fig.1 System hardware configuration

are image segmentation to extract pattern portions, the evaluation and correction of positional displacements of SEM images, the extraction of defects and defect feature specification. The thresholding approach proposed here runs in the UIP.

### 3 PROBLEMS IN THRESHOLDING

SEM images include high-brightness regions around pattern edges due to the edge effect. Consequently, the histogram of each image includes regions with much higher brightness than the average brightness of the actual pattern portions. Let's call these regions edge-effect regions. In addition, multi-modal distribution of more than two peaks can occur in the histogram depending on the mask pattern configuration. This complicates thresholding.

A typical example of a histogram is schematically shown in Fig. 2. The almost flat plateau indicated by c and hill d represent the cumulative edge brightness distribution caused by the edge effect. Since c and d are dependent on the mask structure and the SEM probing condition, they do not always have the same shape. For instance, c will sometimes be a large, smoothly contoured hill instead of a plateau. This tendency of edge-effect region c to change shape makes it difficult to distinguish it from other regions. The small bump e is a part of c. Hills a and b correspond to the cumulative brightness distributions of background and pattern portions, respectively. The positions of these two hills, especially hill b, shift image by image due to changes in the electron charge-up distribution on the mask, so the threshold level must be estimated for every local SEM image. The other more serious problem is that hill a often divides into two or three smaller hills as shown by a1 and a2 in the figure. In addition, hill b often has a sub-peak protruding from its left slope due to the edge effect. The positions of thl and thh are the lowest and highest thresholds and the region between them is the allowance region. Even small errors in thl and thh often lower defect detection accuracy and reliability.

To summarize, the problems in thresholding are how to discriminate hill d and plateau c while taking bumps like e into account; how to discriminate hills a and b and to determine the positions of thl and thh from them; how to know whether hill a or b even exists when their height is as low as plateau c; and how to estimate the extent of hill splitting if it occurs.

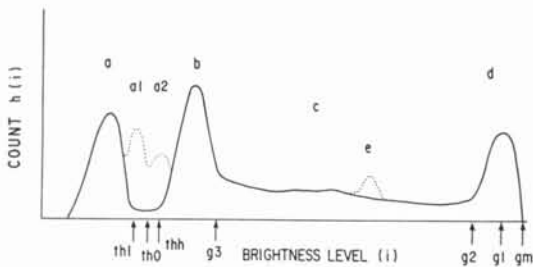


Fig. 2 Schematic of a histogram of an image

### 4 ANALYSIS OF HISTOGRAMS

The thresholding problems described above can be overcome by iteratively analyzing the shape of the histogram of each image. The modules for the shape analysis are iteratively executed under various condition parameters. When the predetermined criteria for reliable thresholding are not satisfactory, the condition parameters are changed and the modules are executed again. This is repeated until the criteria are all satisfied.

Hills a, b and d and plateau c in Fig. 2 are hereafter called label groups a to d. Peaks, valleys and the left and right foots of the hills are labeled p, q, l and h. These are called sublabels. Each label is composed of the label group and sublabels. The features of each label are extracted and standard condition parameters for that label are determined from those features. Some of the features are the height, the gradient, the ratio of the top and valley, the width of each hill and the spacing between adjacent hills. This process is done using samples of typical input SEM images before the automatic inspection starts. If the mask to be inspected has the same mask structure as that of the preceding mask, the condition parameters used for the preceding inspection are used again. After the condition parameters are determined, automatic inspection begins.

Feature positions in the histogram of each input image are extracted together with the features of each position. Thus, the thresholding problem is the correspondence problem between the feature positions and the labels. Figure 3 shows an example of correspondence on a search plane [6]. The bold line represents the correspondence search and the dotted line represents the connection among main label groups a, b, c and d. One constraint is that feature positions in the histogram of a SEM image correspond to the label groups in order of a, b, c and d. The folds in the line in regions b' and e represent the existence of multiple hills in each region. Some feature positions are neglected without matching. Figure 4 schematically shows the modules for thresholding. Hill-search modules C, D and E are for finding plateau c and hills d and e, and main-hill modules A and B are for locating hills a and b. These modules are usually executed from left to right in order. In these modules, the features of feature positions in the histogram calculated from each input image are compared with the condition parameters. The histogram sometimes has a complicated shape and many small hills, which may bring about mismatching. To overcome this problem, a measure of the probability of mismatching is estimated as the cost of the correspondence in each module. The measure is given by the difference of the features from the condition parameters. Matching candidates are extracted in order of the lower cost. If none of the costs are allowable, the condition parameters are changed and the module is executed again.

The next step is to select the true correspondence among the matched candidates. This is done by selecting the correspondence that

satisfies several criteria. One is that all the costs calculated in the modules must be smaller than the allowable limit determined in advance. Other criteria are that the total cost must be smaller than the predetermined value and that the orders of the label groups and the feature positions must be equal. Another important criterion is that the separability showing how well hills a and b can be distinguished must be high. It is estimated in module T along with the threshold level using the discrimination analysis method [7]. When hills a and b are not distinguished correctly or when dominant hill splitting occurs in hill b, the calculated separability is lower than a given allowable value. The other criterion is that when the CAD pattern can be used for thresholding, the calculated threshold has to be within the threshold expectation region. We can calculate the ideal threshold from the occupation ratio of pattern and background portions in the CAD pattern assuming that none of actual defects exist. However, the calculated value often has

large errors for SEM images because parts around the edges of background portions in the CAD pattern are observed as pattern portions in SEM images. Considering this fact, we deduce where the threshold should lie. The region is rather wide to allow for a margin of region estimation error of plateau c. After the criteria are applied in the way described above, the correspondence that satisfies all the criteria and has as lowest cost possible is selected among the candidates. If the criteria can not be satisfied, they are lightened and the condition parameters are changed. Then the above processes are done again from the start.

## 5 RESULTS

An X-ray mask sample with four 4x4mm chips was used in the experiments. It is composed of a silicon nitride thin film a few microns in thickness and a partial tantalum deposit on the film. In this sample, brighter portions of input SEM images correspond to background parts of designed pattern, so brighter and darker levels are reversed in ADP so that brighter portions in the revised images correspond to pattern portions of design data. An example of inspection results is shown in Fig. 5. The resolution of the image is  $0.05 \mu\text{m}/\text{pixel}$ . Figure 5(a) shows the reversed SEM image, in which the especially dark regions at pattern edges are due to the edge effect, (b) is the binarized image thresholded by the proposed approach and (c) shows defects detected by the comparison between the binarized image and the corresponding CAD pattern. The image regions having the brightness between the lower and higher thresholds and those around edges where edge boundaries cannot be exactly distinguished due to the edge effect are

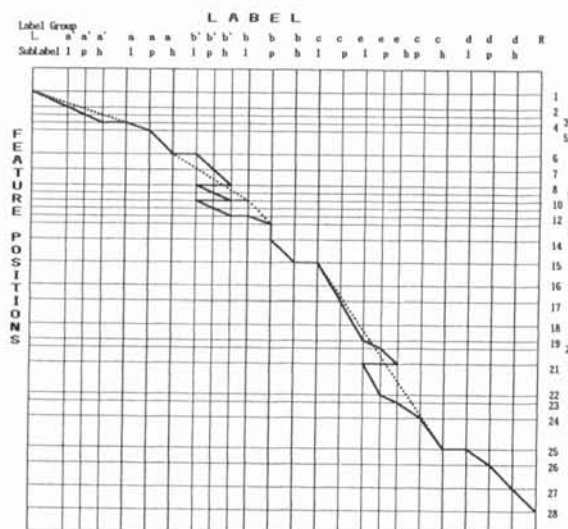


Fig.3 An example of correspondence on a search plane

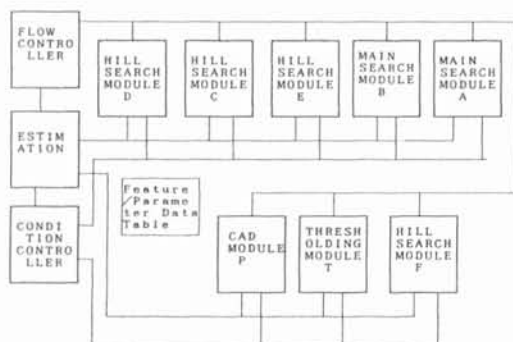


Fig.4 Modules for thresholding

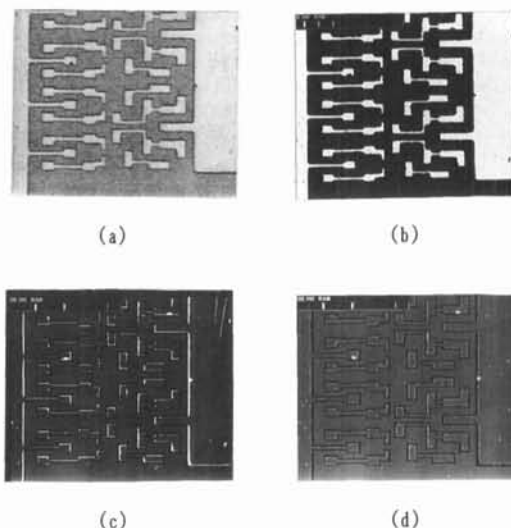


Fig.5 Example of inspection results for a mask sample pattern including random defects, erroneous pattern widths and some missing patterns

considered as ambiguous regions and are neglected. Many edge defects caused by the proximity effect peculiar to electron beam drawing in mask production are clearly detected in (c). The long and fat edge defects shown by the solid and broken lines are due to both the proximity effect and inappropriate etching conditions. Besides these systematically generated erroneous pattern widths, some randomly generated 0.05- $\mu\text{m}$  pinhole defects are detected. Defects larger than 0.1  $\mu\text{m}$  that remained after 2-pixel filtering was applied are shown in (d). They are attributable to electron beam shot error in pattern drawing processes.

## 6 DISCUSSIONS

X-ray mask defects can be classified into two groups according to how defects are generated. The first includes randomly generated defects such as pinholes due to dust on the mask, larger defects due to intermixed contamination, edge positional fluctuations due to electron beam drift and missing patterns due to electron beam shot error in EB lithography. The second includes systematically generated defects such as erroneous widths and positions due to the proximity effect and inappropriate pattern etching conditions in EB lithography as well as missing patterns due to EB data conversion error. To ascertain the quality of a mask, both randomly generated defects and systematically generated ones must be detected. Systematically generated defects commonly occur in all chips, tending to reappear at the same position, and can only be detected by chip-to-CAD comparison. Further, the chip size will greatly increase in the near future to the point where one chip occupies one mask by itself. From these points of view, a thresholding approach for chip-to-CAD comparison is highly desired in the field of LSI production.

Histogram patterns tend to change depending on the SEM beam condition and mask structure, so the condition parameters and criteria are empirically adjusted to the beam condition and mask structure every time they are changed.

When the histogram does not include any noisy hills or dominant edge effect regions, it may be possible to apply the p-tile method to determine the threshold. Actual histograms are, however, too complicated to apply the method with confidence. Many examples were observed where the method caused wrong thresholding. It is especially unreliable when relatively large defects exist in the mask, when the edge effects are rather large or when the hill splitting occurs. Therefore, the CAD data are utilized only to confirm the thresholds calculated in our approach.

The histogram has only a mono-modal shape when the whole region has only a pattern or background portion. In this case, to determine which portion the region has, the corresponding CAD pattern or the result for the overlapped regions of the preceding image is used. On the other hand, when the occupation ratio of the pattern or background portions is very small, the corresponding hill is very low and can be taken as noise. In this case, another main

hill is explicit and the foot of either side can be clearly found because the edge region is small. So, after the threshold is calculated by the discrimination analysis method, the right foot and the calculated threshold are taken as the lower and higher thresholds.

The proposed approach deals with SEM images of samples containing insulator structures that badly deteriorate the image because of dominant electron charge-up. This enables us to inspect not only mask/wafer but also resist wafers and silicon oxide pattern wafers. This is important because inspection by chip-to-CAD comparison for samples with such structures was thought till now to be totally impossible owing to the deterioration mentioned above.

## 7 CONCLUSION

Thresholding problems - the most serious ones in defect detection algorithms - can be solved by iteratively analyzing the shape of the histogram until the criteria become satisfactory for finding the true threshold level of each deteriorated image peculiar to SEM images. This strategy enables the true threshold level to be obtained without mistakes even for the sample having the dominant electron charge-up on the surface. Results obtained with the proposed approach in a practical automated inspection system confirm it provides reliable defect detection. This approach represents a significant advance in the visual inspection, especially in X-ray mask/wafer inspection, which will be of vital importance in near future high-density LSI production.

### ACKNOWLEDGEMENT

This work was at NTT LSI laboratories. The author would like to thank M. Sekimoto of NTT for fabrication of X-ray mask samples. Thanks also to S. Ishihara, A. Shibayama, H. Tsuyuzaki and A. Shindo for useful discussion and to K. Utashiro for collecting inspection data.

### REFERENCES

- (1) D. Fleming, "Prospects for x-ray lithography," *J. Vac. Sci. Tech.*, B, Vol. 10, No. 6, pp. 2511-1511, 1992
- (2) A. Moel, W. Chu, K. Early, Y. C. Ku, E. E. Moon, F. Tsai and H. I. Smith, "Fabrication and characterization of high-flatness mesa-etched silicon nitride x-ray masks," *J. Vac. Sci. Tech.*, B, Vol. 9, No. 6, pp. 3287-3291, Nov/Dec. 1991
- (3) C. W. Jurgensen, R. R. Kola, A. E. Novembre, W. W. Tai, J. Frackoviak, L. E. Trimble and G. K. Celler, "Tungsten patterning for 1:1 x-ray masks," *J. Vac. Sci. Tech.*, B, Vol. 9, No. 6, pp. 3280-3286, Nov/Dec. 1991
- (4) H. Yoda, Y. Ohuch, Y. Taniguchi and M. Ejiri, "An automatic wafer inspection system using pipelined image processing techniques," *IEEE Trans. Patt. Anal. Mach. Intell.*, Vol. 10, No. 1, pp. 4-16, Jan. 1988
- (5) C. W. Oatrey, *The scanning electron microscope*, Cambridge University Press, 1972
- (6) Y. Ohta, Y. Masai and K. Ikeda, "Interval matching method of stereo images using dynamic programming," *IEICE Trans.*, Vol. J68-D, No. 4, pp. 554-561, 1985 (in Japanese)
- (7) N. Ohtsu, "A threshold selection method from gray-level histogram," *IEEE Trans. Sys. Man. Cyber.*, Vol. SMC-9, pp. 62-66, 1979